Reactions of the Cumyloxyl and Benzyloxyl Radicals with Tertiary Amides. Hydrogen Abstraction Selectivity and the Role of Specific Substrate-Radical Hydrogen Bonding

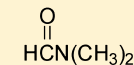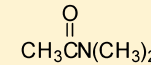Michela Salamone,[†] Michela Milan,[†] Gino A. DiLabio,*[,‡,§] and Massimo Bietti*[,†]

[†]Dipartimento di Scienze e Tecnologie Chimiche, Università "Tor Vergata", Via della Ricerca Scientifica, 1 I-00133 Rome, Italy

[‡]National Institute for Nanotechnology, National Research Council of Canada, 11421 Saskatchewan Drive, Edmonton, Alberta, Canada T6G 2M9

[§]Department of Physics, University of Alberta, Edmonton, Alberta, Canada T6G 2E1

Ⓢ *Supporting Information*

ABSTRACT: A time-resolved kinetic study in acetonitrile and a theoretical investigation of hydrogen abstraction reactions from N,N-dimethylformamide (DMF) and N,N-dimethylacetamide (DMA) by the cumyloxyl (CumO•) and benzyloxyl (BnO•) radicals was carried out. CumO• reacts with both substrates by *direct* hydrogen abstraction. With DMF, abstraction occurs from the formyl and N-methyl C−H bonds, with the formyl being the preferred abstraction site, as

	O‖HCN(CH₃)₂	O‖CH₃CN(CH₃)₂
$k_H(BnO^\bullet)/k_H(CumO^\bullet)$	40	91
k_H/k_D (CumO•)	1.7-5.2	1.3-4.3
k_H/k_D (BnO•)	0.9-1.0	0.8-1.1

indicated by the measured k_H/k_D ratios and by theory. With DMA, abstraction preferentially occurs from the N-methyl groups, whereas abstraction from the acetyl group represents a minor pathway, in line with the computed C−H BDEs and the k_H/k_D ratios. The reactions of BnO• with both substrates were best described by the rate-limiting formation of hydrogen-bonded prereaction complexes between the BnO• α-C−H and the amide oxygen, followed by intramolecular hydrogen abstraction. This mechanism is consistent with the very large increases in reactivity measured on going from CumO• to BnO• and with the observation of k_H/k_D ratios close to unity in the reactions of BnO•. Our modeling supports the different mechanisms proposed for the reactions of CumO• and BnO• and the importance of specific substrate/radical hydrogen bond interactions, moreover providing information on the hydrogen abstraction selectivity.

INTRODUCTION

Hydrogen atom abstraction reactions play a fundamental role in a variety of chemical and biological processes,[1−11] and accordingly considerable attention has been devoted to the study of these reactions. Among the abstracting species, alkoxyl radicals play a prominent role and several aspects of the hydrogen abstraction reactions of these radicals have been investigated in detail.[12−22] Quite surprisingly, little information is presently available on the reactions of alkoxyl radicals with amides, despite the great importance of this class of compounds. For example, amides are widely used as solvents for a variety of purposes in addition to being the main structural feature of peptides and proteins. Time-resolved kinetic studies on the reactions of alkoxyl radicals with amides are limited to a single laser flash photolysis (LFP) study on the reaction of the *tert*-butoxyl radical ((CH₃)₃CO•, *t*BuO•) with N,N-dimethylformamide (DMF) in 2/1 di-*tert*-butyl peroxide/benzene, employing diphenylmethanol as a spectroscopic probe, where a rate constant for hydrogen abstraction (k_H) of 1.0×10^7 M⁻¹ s⁻¹ was measured.[23] k_H values of 5×10^6 and 1.3×10^6 M⁻¹ s⁻¹ were also estimated for hydrogen abstraction from DMF by *t*BuO• and the cumyloxyl radical (PhC(CH₃)₂O•, CumO•), respectively, in DMF.[24,25] Product studies on the reactions of

alkoxyl radicals with amides are also very scarce and are limited to the reactions of *t*BuO•.[26]

Another aspect of great interest is represented by the reaction selectivity, as N,N-dialkylformamides and N,N-dialkylacetamides (and more generally N,N-dialkylalkanamides) can potentially undergo hydrogen abstraction from two different sites, the formyl C−H and the C−H α to the nitrogen in formamides and the C−H α to the nitrogen and to the carbonyl group in acetamides (Scheme 1), and a large number of recently described C−H functionalization procedures based on the reactions of *t*BuO• with tertiary amides provided evidence for highly selective hydrogen abstractions from the formyl C−H bond of formamides and the C−H α to the nitrogen in N,N-dialkylacetamides.[27]
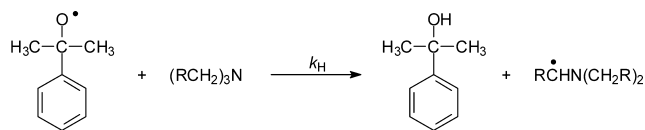
Scheme 1
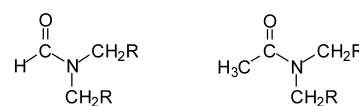
Amides are characterized by relatively high hydrogen bond acceptor (HBA) abilities, as quantitatively expressed by Abraham's β_2^H parameter, which ranges in magnitude from 0.00 for a non-HBA substrate such as an alkane to 1.00 for hexamethylphosphoric acid triamide (HMPA). For DMF and DMA β_2^H = 0.66 and 0.73, respectively, values that are very close to those for alkylamines (β_2^H = 0.58−0.62 for tertiary amines (0.67 for triethylamine) and 0.69−0.73 for primary and secondary amines), indicating comparable HBA abilities for these two classes of compounds.[28]

In this context, we have recently shown that substrate HBA ability can play a very important role in hydrogen abstraction reactions by alkoxyl radicals. Large increases in reactivity were observed on going from CumO• to the benzyloxyl radical (PhCH$_2$O•, BnO•)[29] in their reactions with alkylamines[29] and with substrates characterized by very strong HBA abilities, such as DMSO and HMPA (for which β_2^H = 0.78 and 1.00,[28] respectively).[30] We explained this behavior on the basis of two different mechanisms: the reactions of CumO• were described in all cases in terms of a *direct* hydrogen abstraction mechanism, as shown in Scheme 2 for a generic tertiary amine.

Scheme 2

With BnO•, the kinetic data were rationalized on the basis of a mechanism that proceeds through the formation of a hydrogen-bonded prereaction complex between the BnO• α-C−H and the HBA substrate, wherein hydrogen abstraction occurs (Scheme 3 showing the reaction of BnO• with a generic tertiary amine).[31]

Scheme 3
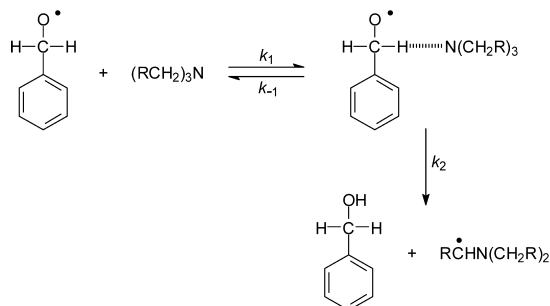
Along these lines, in order to provide quantitative information on the role of structural effects on the hydrogen abstraction reactivity and selectivity of tertiary amides in their reactions with alkoxyl radicals and to probe if substrate−radical hydrogen bond interactions also play a role in the reactions of these substrates with BnO•, we present here the results of a detailed time-resolved kinetic study in acetonitrile solution on the reactions of CumO• and BnO• with N,N-dimethylforma-mide (DMF), N,N-dimethylformamide-d_1 (DMF-d_1), N,N-dimethylformamide-d_6 (DMF-d_6), N,N-dimethylformamide-d_7 (DMF-d_7), N,N-dimethylacetamide (DMA), N,N-dimethylace-tamide-d_3 (DMA-d_3), N,N-dimethylacetamide-d_6 (DMA-d_6),

and N,N-dimethylacetamide-d_9 (DMA-d_9), whose structures are displayed in Chart 1.

Chart 1
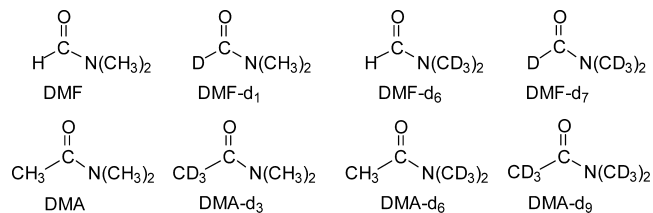

Computational modeling provides additional mechanistic insight into the reactions of CumO• and BnO• with DMF and DMA.

■ RESULTS

The rate constants for the reactions of CumO• and BnO• with the substrates shown in Chart 1 were obtained by laser flash photolysis (LFP). The alkoxyl radicals were generated by 266 nm LFP of nitrogen-saturated acetonitrile solutions (T = 25 °C) containing dicumyl or dibenzyl peroxide, as described in eq 1. In acetonitrile solution, CumO• and BnO• are characterized
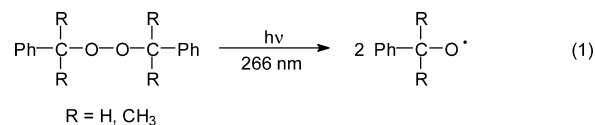
by absorption bands in the visible region of the spectrum centered at 485 and 460 nm, respectively.[32,33] Under these conditions, CumO• decays mainly by C−CH$_3$ β-scission,[22,33] while the decay of BnO• mainly occurs by hydrogen abstraction from the solvent.[34]

The time-resolved spectra observed after reaction of CumO• with DMF and DMA in MeCN solution are reported in the Supporting Information (Figures S1 and S2).

The kinetic studies were carried out by LFP in MeCN solution following the decay of the CumO• and BnO• visible absorption bands at 490 and 460 nm, respectively, as a function of the amide concentration. The observed rate constants (k_{obs}) gave excellent linear relationships when plotted against substrate concentration, and the second-order rate constants for hydrogen abstraction from the substrates (k_H) by the alkoxyl radicals were obtained from the slopes of these plots. As an example, Figure 1 shows the plots of k_{obs} vs [DMF-d_1] for the reactions of this substrate with CumO• (filled circles) and BnO• (open circles) for measurements carried out in acetonitrile at T = 25 °C. The decay curves at different [DMF-d_1] employed for the determination of the k_{obs} values shown in Figure 1 are displayed in the Supporting Information (Figure S3).

Additional plots for hydrogen abstraction from the other amides by CumO• and BnO• are displayed in the Supporting Information (Figures S4−S17). All the kinetic data thus obtained are collected in Table 1 together with the pertinent $k_H(\text{BnO}•)/k_H(\text{CumO}•)$ and k_H/k_D ratios.

■ DISCUSSION

The rate constants associated with the reactions of CumO• are displayed in Table 1. Under the experimental conditions employed, CumO• abstracts a hydrogen atom from DMF with
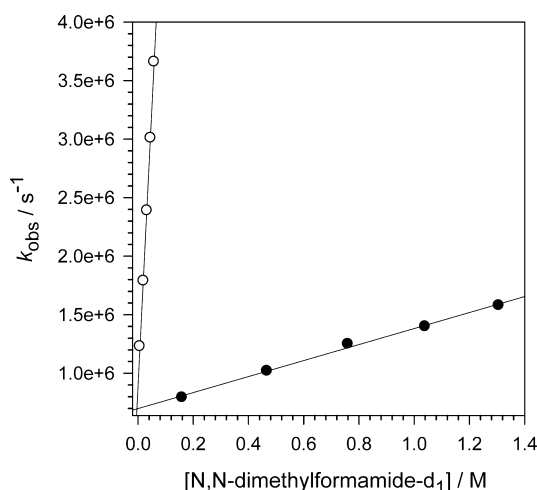
Figure 1. Plots of the observed rate constant (k_{obs}) against [DMF-d_1] for the reactions of the cumyloxyl radical (CumO$^\bullet$, filled circles) and benzyloxyl radical (BnO$^\bullet$, open circles), measured in nitrogen-saturated MeCN solution at T = 25 °C by following the decay of CumO$^\bullet$ and BnO$^\bullet$ at 490 and 460 nm, respectively. From the linear regression analysis: CumO$^\bullet$ + DMF-d_1, intercept 6.99×10^5 s^{-1}, k_H = 6.83×10^5 M^{-1}s^{-1}, r^2 = 0.9962; BnO$^\bullet$ + DMF-d_1, intercept 8.95×10^5 s^{-1}, k_H = 4.73×10^7 M^{-1}s^{-1}, r^2 = 0.9992.

the rate constant k_H = 1.24×10^6 M^{-1} s^{-1}. This value is in reasonable agreement with the available values for hydrogen abstraction from DMF by CumO$^\bullet$ and tBuO$^\bullet$ discussed above.[23−25] An identical value (k_H = 1.24×10^6 M^{-1} s^{-1}) was measured for the reaction between CumO$^\bullet$ and DMA, and, to the best of our knowledge, this represents the first absolute rate constant for hydrogen abstraction from DMA by an alkoxyl radical. The 2 order of magnitude decrease in rate constant observed on going from tertiary alkylamines (for which k_H values between 1×10^8 and 3×10^8 M^{-1} s^{-1} were measured previously)[14,18,20,29,35] to DMF and DMA reflects the important role of polar effects in these reactions. This is in line with the electrophilic character of alkoxyl radicals and with

the more electron-rich C−H bonds of alkylamines in comparison to those of tertiary amides.[36]

The observation of sizable kinetic deuterium isotope effects (KDIEs) in the reactions of CumO$^\bullet$ with DMF (viz., k_H/k_D = 1.8, 1.7, and 5.2 for DMF-d_1, DMF-d_6 and DMF-d_7, respectively) and with DMA (viz. k_H/k_D = 1.3, 2.9, and 4.3 for DMA-d_3, DMA-d_6, and DMA-d_9, respectively) indicates that these reactions can be described as *direct* hydrogen abstractions. Furthermore, these results show that hydrogen abstraction occurs from both the formyl and *N*-methyl C−H bonds in DMF, with the formyl being the preferred abstraction site. Conversely, in DMA abstraction from the acetyl CH$_3$ group represents a minor pathway and the *N*-methyl groups are the preferred abstraction sites. As CumO$^\bullet$ and tBuO$^\bullet$ generally display very similar behaviors in hydrogen abstraction reactions, these results appear to be in partial contrast with the abstraction selectivity observed in synthetic procedures based on hydrogen abstraction from *N,N*-dialkylformamides and *N,N*-dialkylacetamides by tBuO$^\bullet$. In these cases, the exclusive formation of products deriving from abstraction of the formyl C−H and of the C−H bonds that are α to nitrogen, respectively, was described.[27]

Little information is available on the bond dissociation energies (BDEs) of the C−H bonds of DMF and DMA. The available data pertain to the formyl C−H and the C−H bonds that are α to the nitrogen in DMF (BDE = 81.7 and 105 kcal mol^{-1}, respectively) and to the H−CH$_2$CO bond in DMA (BDE = 91.0 kcal mol^{-1}).[37] In all cases the values were not measured directly but were derived from thermochemical cycles or through a correlation.

In order to provide a complete picture of the strength of the different C−H bonds in DMF and DMA, aimed at a better understanding of the factors responsible for the hydrogen abstraction selectivity observed in these reactions, we calculated the BDEs for the C−H bonds of DMF and DMA, using the composite CBS-QB3[38] and W1RO[39] approaches, as implemented in the Gaussian-03 program package.[40] The calculated C−H BDEs for these substrates are displayed in Table 2, together with the available literature values.

Table 1. Second-Order Rate Constants (k_H) and k_H/k_D Ratios Measured for the Reactions of the Cumyloxyl (CumO$^\bullet$) and Benzyloxyl (BnO$^\bullet$) Radicals with Tertiary Amides

substrate	k_H/M^{-1} s^{-1} [a]		k_H(BnO$^\bullet$)/k_H(CumO$^\bullet$)
	CumO$^\bullet$	BnO$^\bullet$	
DMF	$(1.24 \pm 0.02) \times 10^6$	$(5.0 \pm 0.1) \times 10^7$	40
DMF-d_1	$(6.90 \pm 0.06) \times 10^5$	$(4.9 \pm 0.2) \times 10^7$	71
k_H/k_D	1.8	1.02	
DMF-d_6	$(7.47 \pm 0.05) \times 10^5$	$(4.86 \pm 0.02) \times 10^7$	65
k_H/k_D	1.7	1.03	
DMF-d_7	$(2.4 \pm 0.1) \times 10^5$	$(5.45 \pm 0.06) \times 10^7$	227
k_H/k_D	5.2	0.92	
DMA	$(1.24 \pm 0.03) \times 10^6$	$(1.13 \pm 0.02) \times 10^8$	91
DMA-d_3	$(9.5 \pm 0.2) \times 10^5$	$(1.02 \pm 0.03) \times 10^8$	107
k_H/k_D	1.3	1.11	
DMA-d_6	$(4.3 \pm 0.3) \times 10^5$	$(1.2 \pm 0.1) \times 10^8$	279
k_H/k_D	2.9	0.94	
DMA-d_9	$(2.9 \pm 0.1) \times 10^5$	$(1.4 \pm 0.1) \times 10^8$	483
k_H/k_D	4.3	0.81	

[a]Measured in N$_2$-saturated acetonitrile solution at T = 25 °C employing 266 nm LFP: [dicumyl peroxide] = 10 mM or [dibenzyl peroxide] = 8 mM. k_H values were determined from the slope of the k_{obs} vs [substrate] plots, where in turn k_{obs} values were measured following the decay of the CumO$^\bullet$ or BnO$^\bullet$ visible absorption bands at 490 and 460 nm, respectively. Average of at least two determinations.

Table 2. Calculated and Experimental C−H Bond Dissociation Energies (BDEs) for DMF and DMA (kcal mol^{-1})

| | | BDE | | |
| | | calcd | | |
molecule	C−H bond[a]	CBS-QB3	W1RO	lit.[b]
HCON(CH$_3$)$_2$ (DMF)	H−CO	95.0	94.7	81.7
	α-C−H (trans)	94.7	94.0	105
	α-C−H (cis)	94.8	93.9	
CH$_3$CON(CH$_3$)$_2$ (DMA)	H−CH$_2$CO	99.6		91.0
	α-C−H (trans)	92.5		
	α-C−H (cis)	94.1		

[a]cis and trans refer to the stereochemical relationship between the N-methyl group and the C=O bond. [b]Reference 37.

In general, the composite methods we used to compute the C−H BDEs in DMF and DMA are known to be fairly reliable for this purpose.[30,41] The consistency of the BDEs predicted by the methods, coupled with the reliability of the computational methods, provides us with a good deal of certainty regarding our calculated values. We offer that our computed BDE values for the different C−H bonds in DMF and DMA are likely to be closer to the true values than the presently available literature values. The very similar calculated BDEs for the H−CO and NCH$_2$−H bonds of DMF and the significantly higher BDE value calculated for the H−CH$_2$CO bond as compared to the NCH$_2$−H bonds of DMA are in agreement with the hydrogen abstraction selectivities discussed above for the reactions of CumO$^\bullet$ with DMF and DMA, derived from the measured KDIEs.

The kinetic data displayed in Table 1 clearly show that, with both substrates, very large increases in k_H occur on going from CumO$^\bullet$ to BnO$^\bullet$, as quantitatively demonstrated by the k_H(BnO$^\bullet$)/k_H(CumO$^\bullet$) ratios that vary between 40 and 483 for the reactions studied. This behavior is consistent with the relatively strong HBA ability of DMF and DMA (β_2^H = 0.66 and 0.73, respectively)[28] and the previously described strong hydrogen bond donor (HBD) ability of BnO$^\bullet$.[34] Accordingly, the reactions of BnO$^\bullet$ with these substrates can be described in terms of the formation of hydrogen bonded prereaction complexes between the BnO$^\bullet$ α-C−H and the amide oxygen, followed by intramolecular hydrogen atom transfer within the complex, in analogy to previously described reactions of BnO$^\bullet$ with substrates characterized by strong to very strong HBA abilities, such as alkylamines, DMSO, and HMPA.[29,30,42] Scheme 4 displays the mechanism for the reaction of BnO$^\bullet$ with DMF, where hydrogen abstraction can occur from the H−CO and/or NCH$_2$−H bonds (vide infra). k_1 and k_{-1} represent
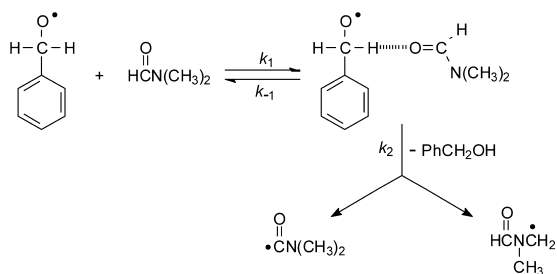
the rate constants for the formation and dissociation of the prereaction complex, and k_2 is the rate constant for intramolecular hydrogen abstraction within the complex.

The observation of k_H/k_D ratios very close to unity in the reactions of BnO$^\bullet$ with DMF, DMF-d_1, DMF-d_6, and DMF-d_7 provides support to this mechanism by indicating that C−H bond cleavage does not occur in the rate-determining step of the reaction, as previously described for the reactions of BnO$^\bullet$ with triethylamine/triethylamine-d_{15}, DMSO/DMSO-d_6, and HMPA/HMPA-d_{18}.[29d,30] On the basis of this picture, $k_2 \gg k_{-1}$ reasonably applies and the reaction rate can be expressed in terms of the rate constant for complex formation k_1 as $v = k_1$ [substrate][BnO$^\bullet$], where k_1 corresponds to the measured k_H values displayed in Table 1 for the reactions of BnO$^\bullet$. A similar behavior is also observed in the reactions of BnO$^\bullet$ with DMA, DMA-d_3, DMA-d_6, and DMA-d_9. Therefore, the increase in k_H observed on going from DMF to DMA (k_H = 5.0 × 10^7 and 1.13 × 10^8 M^{-1} s^{-1}, respectively) can be explained on the basis of the corresponding increase in substrate HBA ability (β_2^H = 0.66 and 0.73 for DMF and DMA, respectively), i.e. of the formation of a relatively stronger substrate/radical prereaction complex for DMA in comparison to DMF (see later).

We obtained additional support for the different hydrogen abstraction mechanisms involving CumO$^\bullet$ and BnO$^\bullet$ from quantum chemical modeling. We performed simulations of the prereaction complex and transition state structures associated with the reactions of CumO$^\bullet$ and BnO$^\bullet$ with DMF and DMA with the B3LYP/6-31+G(2d,2p)[44,45] density functional theory (DFT). In conjunction with this approach, we employed dispersion-correcting potentials (DCPs) to more accurately capture noncovalent interactions.[46] Owing to the presence of different C−H bonds in both DMF and DMA, several pathways associated with hydrogen abstraction could be taken. Rather than provide the details of the many possible reaction paths, we present here calculated data associated with only the lowest energy pathways we were able to find for abstraction from each unique site of the two substrates. These data are collected in Table 3.

The data in Table 3 for the reaction of CumO$^\bullet$ with DMF are consistent with the experimentally observed rate constants and KDIEs presented in Table 1 and the calculated BDEs given

Scheme 4

Table 3. Calculated Free Energy Barrier Heights ($\Delta G^\ddagger$, kcal mol^{-1}) and Rate Constants for Direct Hydrogen Atom Abstraction from Different C−H Bonds in DMF and DMA by CumO$^\bullet$ and BnO$^\bullet$

| reaction	abstraction site	$\Delta G^\ddagger$	k_{calcd} (M^{-1}s^{-1})	k_{exptl} (M^{-1}s^{-1})[a]
CumO$^\bullet$ + DMF	trans N-methyl	10.1	2.6 × 10^5	
	cis N-methyl	10.6	1.1 × 10^5	
	formyl	8.0	7.9 × 10^6	1.24 × 10^6
CumO$^\bullet$ + DMA	trans N-methyl	8.8	2.4 × 10^6	
	cis N-methyl	9.1	1.4 × 10^6	
	acetyl	13.9	4.1 × 10^2	1.24 × 10^6
BnO$^\bullet$ + DMF	trans N-methyl	11.2	4.2 × 10^4	
	cis N-methyl	11.3	3.5 × 10^4	
	formyl	8.8	2.4 × 10^6	5.0 × 10^7
BnO$^\bullet$ + DMA	trans N-methyl	9.6	6.0 × 10^5	
	cis N-methyl	9.7	5.2 × 10^5	
	acetyl	15.3	8.1 × 10^1	1.13 × 10^8

[a]Values from Table 1.
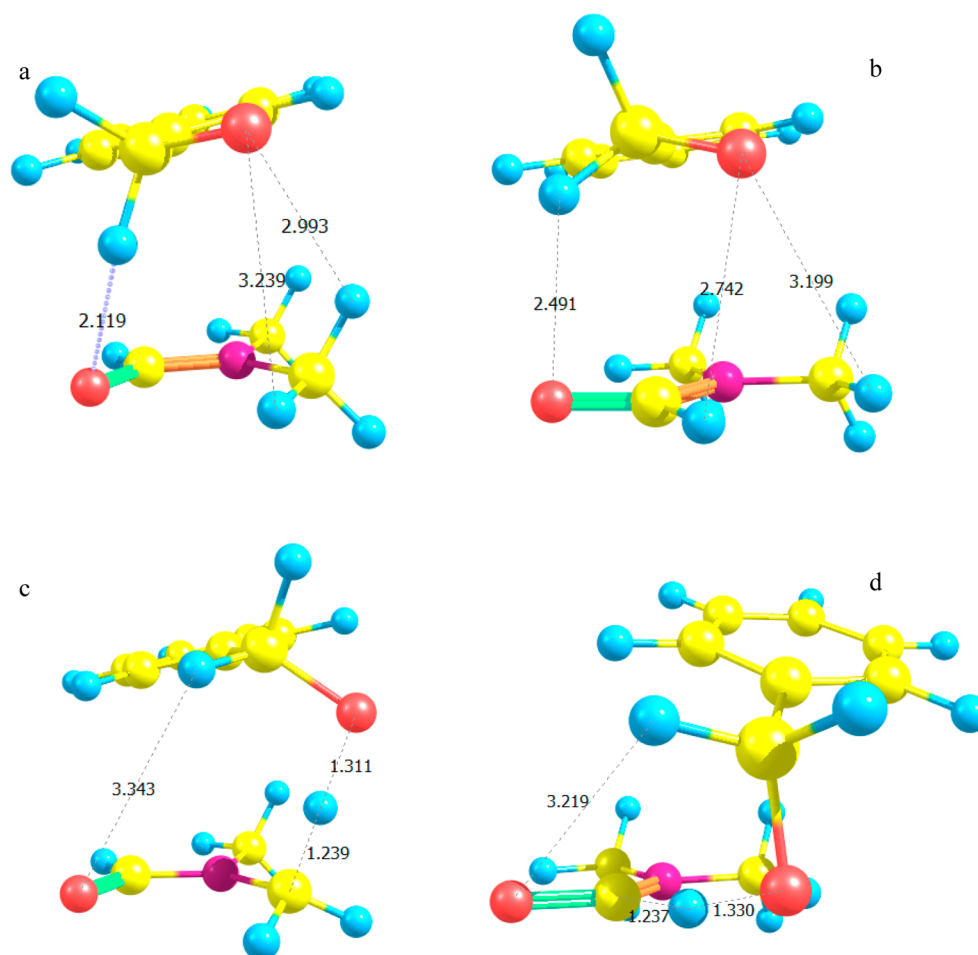
Figure 2. Prereaction (a, b) and transition state (c, d) complexes formed in the reaction of BnO$^\bullet$ and DMF as predicted by simulations. Key interatomic separations (Å) are shown. Calculated binding energies are (a) 8.5 and (b) 7.8 kcal mol^{-1}. The energy/free energy barriers to reach the transition state complexes from the prereaction complexes are as follows: (c) from (a), 8.0/7.5 kcal mol^{-1}; (d) from (b), 5.0/4.4 kcal mol^{-1}. Color key: red, O; purple, N; yellow, C; light blue, H.

in Table 2. For example, the BDE data indicate that the most easily abstracted hydrogen atom in DMF is the formyl atom and we find that the lowest free energy barrier to hydrogen abstraction is associated with this site. The computed rate constants show that abstraction from the formyl site, viz. 7.9 × 10^6 M^{-1} s^{-1}, is in reasonable agreement with the experimentally determined value of 1.24 × 10^6 M^{-1} s^{-1}. The calculations suggest that abstraction from both of the *N*-methyl groups might occur, but at rates that are more than 1 order of magnitude lower than that associated with abstraction from the formyl group.

The acetyl hydrogen in DMA is predicted by calculations to be much more difficult to abstract than the formyl hydrogen in DMF. This result nicely agrees with the computed BDEs, which indicate that the acetyl C−H BDE is more than 5 kcal mol^{-1} larger than the *N*-methyl C−H BDEs. Abstractions from either of the *N*-methyl groups have computed barriers that are 4−5 kcal mol^{-1} lower than that associated with abstraction from the acetyl group and corresponding computed rate constants of (1.4−2.4) × 10^6 M^{-1} s^{-1} that are in good agreement with the measured value.

The good agreement in the reactivity of CumO$^\bullet$ is starkly contrasted by the poorly predicted rate constants associated with the BnO$^\bullet$ reactions. Specifically, the predicted barrier heights for the abstraction of the hydrogen atoms of DMF and

DMA range from 8.8 to 11.3 kcal mol^{-1}. These barriers lead to rate constants that are in all cases from 1 to 6 orders of magnitude lower than those measured experimentally. We propose that the considerable underestimation of the BnO$^\bullet$ rate constants for *direct* hydrogen abstraction supports the notion that this radical does not react by a *direct* hydrogen abstraction mechanism but has kinetics that are controlled by prereaction complex formation, as previously described for the reactions of this radical with strong HBA substrates.[29,30]

We performed additional simulations in order to explore the details of the formation of prereaction complexes involving BnO$^\bullet$ and the substrates. In Figure 2, we show the lowest energy (enthalpy) structures in which the abstracting oxygen atom is oriented toward the *N*-methyl (Figure 2a) and formyl (Figure 2b) of DMF.

The prereaction complexes are quite strongly bound, with binding energies (BEs) as high as 8.5 kcal mol^{-1}.[47] The binding in the complexes is due to hydrogen bonding between the benzylic C−H group in BnO$^\bullet$ and the oxygen atom in DMF. Additional interactions occur between the BnO$^\bullet$ oxygen atom and the formyl and/or *N*-methyl hydrogen atoms, in addition to nonspecific π stacking. The hydrogen bond interactions orient the abstracting oxygen atom such that it is in close proximity to labile hydrogen atoms in the DMF substrate (see Figure 2a,b for some key interatomic distances). It does not
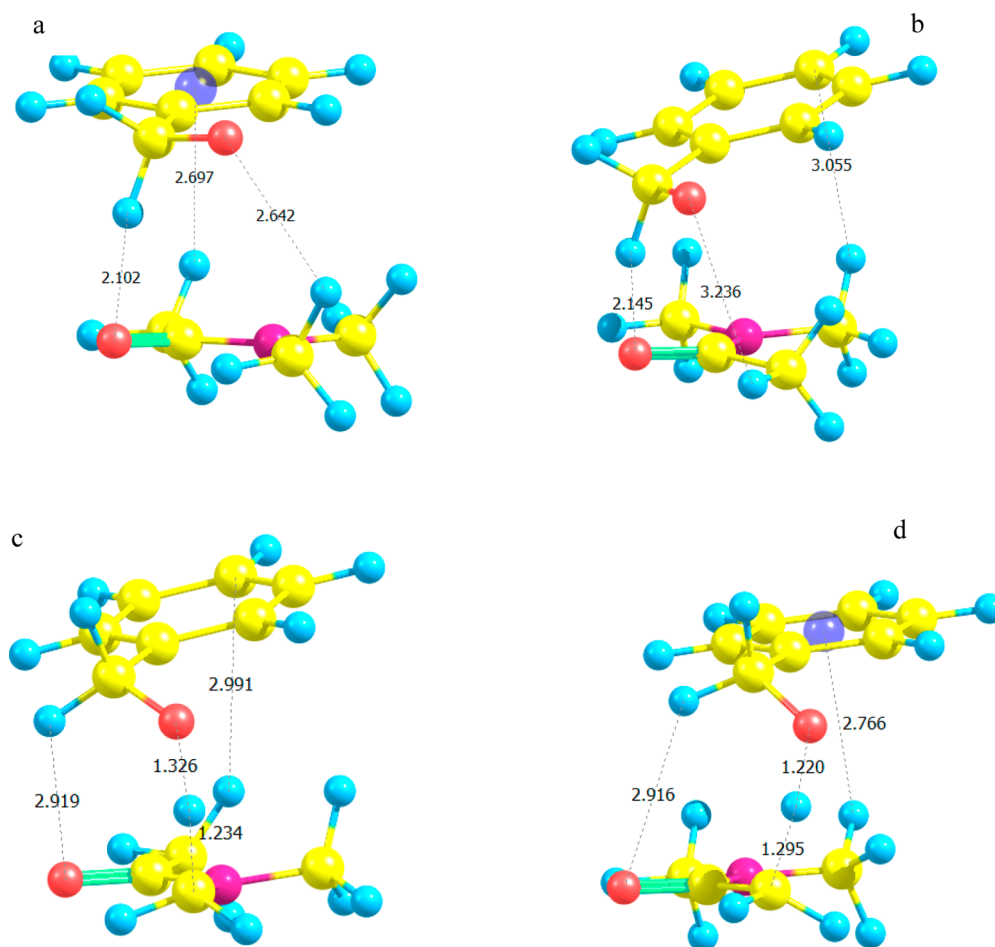
Figure 3. Prereaction (a, b) and transition state (c, d) complexes formed in the reaction of BnO$^\bullet$ and DMA as predicted by simulations. Key interatomic separations (Å) are shown. Calculated BEs are (a) 9.5 and (b) 8.8 kcal mol^{-1}. The energy/free energy barriers to reach the transition state complexes from the prereaction complexes are as follows: (c) from (a), 6.9/5.7 kcal mol^{-1}; (d) from (b), 12.8/10.4 kcal mol^{-1}. Color key: red, O; purple, N; yellow, C; light blue, H; transparent dark blue, ring center.

appear possible for (BnO$^\bullet$)OCH···O(DMF) to be maintained in conjunction with a (BnO$^\bullet$)OCH···HC(*trans*)N(DMF) interaction, nor did we find any low-energy complexes in which there are simultaneous (BnO$^\bullet$)OCH···N(DMF) and (BnO$^\bullet$)OCH···HCN(*trans*)(DMF) interactions. This implies that in the reaction between BnO$^\bullet$ and DMF abstraction may not occur from the *trans* N-methyl group.

An evaluation of the Boltzmann populations of the prereaction complexes based on binding enthalpies indicates that ca. 67% of the complexes take the form shown in Figure 2a, while the form shown in Figure 2b makes up ca. 20% of the population.

The strength of binding and the specific hydrogen bond interactions in these complexes provide good support to the idea that they play an important role in the abstraction process and that there is little selectivity between the formyl and the *cis* N-methyl hydrogen atoms in the reaction.

The lowest energy prereaction complex (Figure 2a) can reach the transition state (TS) complex shown in Figure 2c, which illustrates a hydrogen abstraction from the *cis* N-methyl group. This TS complex can be reached by surmounting an energy (free energy) barrier of 8.0 (7.5) kcal mol^{-1}, which involves stretching the (BnO$^\bullet$)OCH···O(DMF) hydrogen bond in the prereaction complex and better formation of a weaker (BnO$^\bullet$)HCO···HCN(DMF) interaction. The stacking

interaction between the π systems of the reactants is maintained from the prereaction complex to the TS. The computed rate constant associated with this reaction pathway is 2.0×10^7 s^{-1}, which represents the *intrinsic* rate constant, k_H', for intramolecular hydrogen abstraction within the complex.[30]

The prereaction complex shown in Figure 2b can reach TS structures involving the abstraction of the formyl and N-methyl hydrogen atoms, with the former shown in Figure 2d. Abstraction of the formyl hydrogen atom has a calculated energy (free energy) barrier of 5.0 (4.4) kcal mol^{-1}. To reach this TS requires stretching the (BnO$^\bullet$)OCH···O(DMF) hydrogen bond of the prereaction complex while forming a new (BnO$^\bullet$)HCO···HCO(DMF) hydrogen bond. The formation of this TS also involves the loss of the stacking interaction between the reactants. The relatively low barrier of this process reflects the fact that hydrogen bond interactions are dominant over π stacking. The computed k_H' for this process (i.e., that represented by Figure 2b → Figure 2d) is 4.0×10^9 s^{-1}. This result suggest that facile abstraction occurs from the formyl site; however, the contribution of this reaction pathway to the overall rate constant is reduced by the lower population of the prereaction complex shown in Figure 2b.[48]

Weighing the computed rate constants for the reaction of BnO$^\bullet$ with DMF according to the Boltzmann distributions of the prereaction complexes gives a value $k_H' = 1.3 \times 10^9$ s^{-1}.

This value can be compared with the k_H' value derived for the reaction between BnO$^{\bullet}$ and DMSO ($k_H' = 1.5 \times 10^7$ s^{-1}), where experimental evidence for pre-equilibrium kinetics was obtained and the measured second-order rate constant (k_H) was shown to be a composite of k_H' and of the preequilibrium constant.[30]

In an attempt to obtain an experimental k_H' value for the reaction of BnO$^{\bullet}$ with DMF, the kinetic study of this reaction was extended to significantly higher DMF concentrations ([DMF] ≤ 0.25 M) in comparison to the experiment shown in the Supporting Information (Figure S11), whose results are displayed in Table 1. However, no deviation from linearity was observed under these conditions. This observation clearly indicates that the k_H' value for the reaction of BnO$^{\bullet}$ with DMF must be significantly higher than the value obtained for the corresponding reaction with DMSO,[30] which is in full agreement with the calculated value. This large difference in intrinsic hydrogen abstraction reactivities reasonably reflects the significantly higher BDE for the C−H bonds of DMSO in comparison to DMF (102.1[30] and 94−95 kcal mol^{-1} for DMSO and DMF (see Table 2), respectively).

For the reaction of BnO$^{\bullet}$ with DMA, several energetically low-lying prereaction complexes are formed. As is the case for BnO$^{\bullet}$-DMF, complexes involving BnO$^{\bullet}$ and DMA are dominated by the interaction of the OCH moiety of the radical with the oxygen atom of the substrate. Secondary interactions between DMA *cis* N-methyl C−H groups and the oxygen atom and aromatic ring of BnO$^{\bullet}$ also occur.

We were unable to find a complex in which the BnO$^{\bullet}$ oxygen atom was oriented close to a DMA *trans* N-methyl hydrogen atom. Figure 3a shows the most strongly bound BnO$^{\bullet}$−DMA prereaction complex, which has a binding energy (enthalpy) of 9.5 (7.9) kcal mol^{-1}, and Figure 3b shows a slightly weakly bound structure having a binding energy (enthalpy) of 8.8 (7.2) kcal mol^{-1}. In these cases, the slightly higher binding energies relative to that predicted for the BnO$^{\bullet}$−DMF complexes is consistent with the additional dispersion interactions that occur as a result of the presence of the methyl group in DMA. This methyl also contributes electron density to the carbonyl group, thus increasing its HBA ability ($\beta_2^H = 0.66$ and 0.73 for DMF and DMA, respectively).[28]

The structure shown in Figure 3a appears to favor hydrogen abstraction from the *cis* N-methyl group, as shown in Figure 3c. According to our calculations, the energy (free energy) barrier to this reaction is 6.9 (5.7) kcal mol^{-1}, which translates into a k_H' value of 5.4×10^8 s^{-1}. For the abstraction process illustrated by Figure 3b → Figure 3d, the energy (free energy) barrier is significantly higher, being 12.8 (10.4) kcal mol^{-1}. This is consistent with the much higher (calculated) BDE associated with a C−H moiety of the acetyl group in comparison to an N-methyl value. The calculated rate constant for this abstraction is correspondingly low, at 1.5×10^5 s^{-1}, which suggests that within the prereaction complex abstraction from this site does not compete to any significant extent.

CumO$^{\bullet}$ is capable of interacting noncovalently with DMF and DMA. However, this radical does not have a strong hydrogen bond donating group; therefore, interactions are expected to be dominated by nonspecific stacking interactions and weak, secondary interactions involving the radical oxygen center as a HBA moiety. The lack of strong interactions that favorably orient the abstracting oxygen with labile hydrogen atoms on the substrates implies that prereaction complex formation plays a less important role in comparison to the corresponding reactions involving BnO$^{\bullet}$. We explored this to a significant extent by computing the energies of a number of different radical−substrate complexes and of hydrogen abstraction transition state structures, as well as potential energy surfaces associated with laterally displacing the radical with respect to the substrate. These data are collected in the Supporting Information (Figures S18−S21), and we present here a summary of our findings. Our calculations predict that the binding energies of CumO$^{\bullet}$ to DMF and DMA are up to 1.5 kcal mol^{-1} lower than in complexes involving BnO$^{\bullet}$. This difference incorporates a reduction in binding energy as a result of the absence of HBD moieties in the radical and enhancements through additional dispersion-type binding afforded to CumO$^{\bullet}$ by the presence of methyl groups. Furthermore, the "softer" potential energy surfaces associated with CumO$^{\bullet}$−DMA binding (as shown in the Supporting Information, Figure S21) in comparison to those for BnO$^{\bullet}$−DMA complexes demonstrate that the lack of specific binding between reactants prevents efficient intramolecular hydrogen abstraction.

In conclusion, by means of time-resolved kinetic studies and quantum mechanical modeling we have provided detailed information on the hydrogen abstraction reactivity and selectivity of the two important tertiary amides DMF and DMA in their reactions with alkoxyl radicals. Reliable BDE values for the different C−H bonds of DMF and DMA have also been obtained. In the reactions of these substrates with CumO$^{\bullet}$ no specific substrate−radical interaction occurs and the reactions have been described as *direct* hydrogen abstractions in full agreement with the measured KDIEs and the computed BDE values. C−H abstraction occurs from the formyl and, to a lesser extent, the N-methyl groups in DMF, and preferentially from the N-methyl groups in DMA, where abstraction from the acetyl CH$_3$ group represents a minor pathway. The large increases in reactivity observed on going from CumO$^{\bullet}$ to BnO$^{\bullet}$ have been explained on the basis of a mechanism that proceeds through the formation of strongly bound prereaction complexes between the relatively acidic α-C−H of BnO$^{\bullet}$ and the amide oxygen followed by intramolecular hydrogen atom transfer, as supported by computational modeling that moreover provides information on the hydrogen abstraction selectivity. These results provide a demonstration of the importance of substrate−radical hydrogen bond interactions in these processes, suggesting that this association may play a role in hydrogen abstraction reactions from peptides and proteins by oxygen-centered radicals. These intriguing aspects are currently under investigation in our laboratory.

■ EXPERIMENTAL SECTION

Materials. Spectroscopic grade acetonitrile was used in the kinetic experiments. N,N-dimethylformamide (DMF), N,N-dimethylformamide-d_1 (DMF-d_1), N,N-dimethylformamide-d_6 (DMF-d_6), N,N-dimethylformamide-d_7 (DMF-d_7), N,N-dimethylacetamide (DMA), N,N-dimethylacetamide-d_3 (DMA-d_3), and N,N-dimethylacetamide-d_9 (DMA-d_9) were of the highest commercial quality available and were used as received. N,N-Dimethylacetamide-d_6 (DMA-d_6) was synthesized according to the following procedure. A 3 g amount (0.0343 mol) of (CD$_3$)$_2$NH·HCl was dissolved in 5 mL of a 7 M NaOH solution. After a few minutes 1.2 mL (0.017 mol) of acetyl chloride was added dropwise. The reaction mixture was stirred at room temperature for 30 min. Water was then added, and the mixture was extracted with dichloromethane (3 × 25 mL). The combined organic extracts were dried over anhydrous NaSO$_4$ and filtered, and the solvent was removed under reduced pressure. The product was

purified by flash column chromatography (silica gel, eluent dichloromethane/methanol 50/1) to give 0.7 g of pure product (GC > 99%, 44% yield), identified by ^{1}H NMR.

Dicumyl peroxide was of the highest commercial quality available and was used as received. Dibenzyl peroxide was prepared according to a previously described procedure by reaction of KO_2 with benzyl bromide in dry benzene, in the presence of 18-crown-6.[49]

Laser Flash Photolysis Studies. LFP experiments were carried out with a laser kinetic spectrometer using the fourth harmonic (266 nm) of a Q-switched Nd:YAG laser, delivering 8 ns pulses. The laser energy was adjusted to ≤10 mJ/pulse by the use of the appropriate filter. A 3.5 mL Suprasil quartz cell (10 mm ×10 mm) was used in all experiments. Nitrogen-saturated solutions of dicumyl peroxide and dibenzyl peroxide (10 and 8 mM, respectively) were employed. All of the experiments were carried out at $T = 25 \pm 0.5$ °C with magnetic stirring. The observed rate constants (k_{obs}) were obtained by averaging three to five individual values and were reproducible to within 5%.

Second-order rate constants for the reactions of the cumyloxyl and benzyloxyl radicals with the amides were obtained from the slopes of the k_{obs} (measured following the decay of the cumyloxyl and benzyloxyl radical visible absorption bands at 490 and 460 nm, respectively) vs [amide] plots. Fresh solutions were used for every amide concentration. Correlation coefficients were in all cases >0.992. The rate constants displayed in Table 1 are the average of at least two independent experiments, typical errors being ≤10%.

Computational Studies. Calculations were performed using B3LYP-DCP/6-31+G(2d,2p) with the Gaussian-03 program package.[40] Vibration frequency calculations verified the correct nature of local minima and transition states. Several initial orientations were used to determine the structures of prereaction complexes, from which transition state structures were determined. The calculations did not take into account the effects of solvent. Rate constants are calculated from transition state theory using the free energy differences between the free reactants and the transition state complexes and the prereaction and transition state complexes.

■ ASSOCIATED CONTENT

Ⓢ Supporting Information

Figures, tables, and texts giving plots of k_{obs} vs substrate concentration for the reactions of CumO[•] and BnO[•], details of the calculations and an input file demonstrating the use of dispersion-correcting potentials, and potential energy surfaces associated with laterally displacing the radical with respect to the substrate. This material is available free of charge via the Internet at http://pubs.acs.org.

■ AUTHOR INFORMATION

Corresponding Author
*E-mail: Gino.DiLabio@nrc.ca (G.A.D.); bietti@uniroma2.it (M.B.).

Notes
The authors declare no competing financial interest.

■ ACKNOWLEDGMENTS

■ REFERENCES

(1) Halliwell, B.; Gutteridge, J. M. C. *Free Radicals in Biology and Medicine*, 4th ed.; Oxford University Press: Oxford, U.K., 2007.

(2) Hanthorn, J. J.; Valgimigli, L.; Pratt, D. A. *J. Am. Chem. Soc.* **2012**, *134*, 8306−8309.

(3) Pratt, D. A.; Tallman, K. A.; Porter, N. A. *Acc. Chem. Res.* **2011**, *44*, 458−467.

(4) Matthews, M. L.; Neumann, C. S.; Miles, L. A.; Grove, T. L.; Booker, S. J.; Krebs, C.; Walsh, C. T.; Bollinger, J. M., Jr. *Proc. Natl. Acad. Sci. U.S.A.* **2009**, *106*, 17723−17728.

(5) Dietl, N.; Schlangen, M.; Schwarz, H. *Angew. Chem., Int. Ed.* **2012**, *51*, 5544−5555.

(6) Lai, W.; Li, C.; Chen, H.; Shaik, S. *Angew. Chem., Int. Ed.* **2012**, *51*, 5556−5578.

(7) Mayer, J. M. *Acc. Chem. Res.* **2011**, *44*, 36−46.

(8) Liu, L. V.; Hong, S.; Cho, J.; Nam, W.; Solomon, E. I. *J. Am. Chem. Soc.* **2013**, *135*, 3286−3299.

(9) Atkinson, R.; Arey, J. *Chem. Rev.* **2003**, *103*, 4605−4638.

(10) Michaudel, Q.; Thevenet, D.; Baran, P. S. *J. Am. Chem. Soc.* **2012**, *134*, 2547−2550.

(11) White, M. C. *Science* **2012**, *335*, 807−809.

(12) Salamone, M.; Mangiacapra, L.; DiLabio, G. A.; Bietti, M. *J. Am. Chem. Soc.* **2013**, *135*, 415−423.

(13) Salamone, M.; Giammarioli, I.; Bietti, M. *J. Org. Chem.* **2011**, *76*, 4645−4651.

(14) Bietti, M.; Salamone, M. *Org. Lett.* **2010**, *12*, 3654−3657.

(15) Kawashima, T.; Ohkubo, K.; Fukuzumi, S. *J. Phys. Chem. B* **2010**, *114*, 675−680.

(16) Cosa, G.; Scaiano, J. C. *Org. Biomol. Chem.* **2008**, *6*, 4609−4614.

(17) Litwinienko, G.; Ingold, K. U. *Acc. Chem. Res.* **2007**, *40*, 222−230.

(18) Finn, M.; Friedline, R.; Suleman, N. K.; Wohl, C. J.; Tanko, J. M. *J. Am. Chem. Soc.* **2004**, *126*, 7578−7584.

(19) Orlando, J. J.; Tyndall, G. S.; Wallington, T. J. *Chem. Rev.* **2003**, *103*, 4657−4689.

(20) Pischel, U.; Nau, W. M. *J. Am. Chem. Soc.* **2001**, *123*, 9727−9737.

(21) Snelgrove, D. W.; Lusztyk, J.; Banks, J. T.; Mulder, P.; Ingold, K. U. *J. Am. Chem. Soc.* **2001**, *123*, 469−477.

(22) Avila, D. V.; Brown, C. E.; Ingold, K. U.; Lusztyk, J. *J. Am. Chem. Soc.* **1993**, *115*, 466−470.

(23) Chatgilialoglu, C.; Lunazzi, L.; Macciantelli, D.; Placucci, G. *J. Am. Chem. Soc.* **1984**, *106*, 5252−5256.

(24) Kjaer, N. T.; Lund, H. *Acta Chem. Scand.* **1995**, *49*, 848−852.

(25) Donkers, R. L.; Maran, F.; Wayner, D. D. M.; Workentin, M. S. *J. Am. Chem. Soc.* **1999**, *121*, 7239−7248.

(26) Costantino, L.; Iley, J. *Org. Biomol. Chem.* **2004**, *2*, 1894−1900. Iley, J.; Tolando, R.; Costantino, L. *J. Chem. Soc., Perkin Trans. 2* **2001**, 1299−1305. Friedman, L.; Shechter, H. *Tetrahedron Lett.* **1961**, *2*, 238−242.

(27) (a) Li, X.; Li, B.; You, J.; Lan, J. *Org. Biomol. Chem.* **2013**, *11*, 1925−1928. (b) Ding, S.; Jiao, N. *Angew. Chem., Int. Ed.* **2012**, *51*, 9226−9237. (c) Yan, Y.; Zhang, Y.; Feng, C.; Zha, Z.; Wang, Z. *Angew. Chem., Int. Ed.* **2012**, *51*, 8077−8081. (d) Xia, Q.; Chen, W. *J. Org. Chem.* **2012**, *77*, 9366−9373. (e) Mai, W.-P.; Wang, H.-H.; Li, Z.-C.; Yuan, J.-W.; Xiao, Y.-M.; Yang, L.-R.; Mao, P.; Qu, L.-B. *Chem. Commun.* **2012**, *48*, 10117−10119. (f) Lao, Z.-Q.; Zhong, W.-H.; Lou, Q.-H.; Li, Z.-J.; Meng, X.-B. *Org. Biomol. Chem.* **2012**, *10*, 7869−7871. (g) Barve, B. D.; Wu, Y.-C.; El-Shazly, M.; Chuang, D.-W.; Chung, Y.-M.; Tsai, Y.-H.; Wu, S.-F.; Korinek, M.; Du, Y.-C.; Hsieh, C.-T.; Wang, J.-J.; Chang, F.-R. *Eur. J. Org. Chem.* **2012**, 6760−6766. (h) He, T.; Li, H.; Li, P.; Wang, L. *Chem. Commun.* **2011**, *47*, 8946−8948.

(28) Abraham, M. H.; Grellier, P. L.; Prior, D. V.; Morris, J. J.; Taylor, P. J. *J. Chem. Soc., Perkin Trans. 2* **1990**, 521−529.

(29) (a) Salamone, M.; Martella, R.; Bietti, M. *J. Org. Chem.* **2012**, *77*, 8556−8561. (b) Salamone, M.; DiLabio, G. A.; Bietti, M. *J. Am. Chem. Soc.* **2011**, *133*, 16625−16634. (c) Salamone, M.; DiLabio, G. A.; Bietti, M. *J. Org. Chem.* **2011**, *76*, 6264−6270. (d) Salamone, M.; Anastasi, G.; Bietti, M.; DiLabio, G. A. *Org. Lett.* **2011**, *13*, 260−263.

(30) Salamone, M.; DiLabio, G. A.; Bietti, M. *J. Org. Chem.* **2012**, *77*, 10479−10487.

(31) Evidence supporting the HBD ability of primary alkoxyl radicals has been recently provided in a study of the reactions of $CH_3O[•]$ and $CH_3CH_2O[•]$ with pyridine bases. See: Shukla, D.; Adiga, S. P.; Ahearn, W. G.; Dinnocenzo, J. P.; Farid, S. *J. Org. Chem.* **2013**, *78*, 1955−1964.

(32) Avila, D. V.; Ingold, K. U.; Di Nardo, A. A.; Zerbetto, F.; Zgierski, M. Z.; Lusztyk, J. *J. Am. Chem. Soc.* **1995**, *117*, 2711−2718.

(33) Baciocchi, E.; Bietti, M.; Salamone, M.; Steenken, S. *J. Org. Chem.* **2002**, *67*, 2266−2270.

(34) Konya, K. G.; Paul, T.; Lin, S.; Lusztyk, J.; Ingold, K. U. *J. Am. Chem. Soc.* **2000**, *122*, 7518−7527.

(35) Griller, D.; Howard, J. A.; Marriott, P. R.; Scaiano, J. C. *J. Am. Chem. Soc.* **1981**, *103*, 619−623.

(36) Roberts, B. P. *Chem. Soc. Rev.* **1999**, *28*, 25−35.

(37) Luo, Y.-R. *Comprehensive Handbook of Chemical Bond Energies*; CRC Press: Boca Raton, FL, 2007.

(38) Montgomery, J. A., Jr.; Frisch, M. J.; Ochterski, J. W.; Petersson, G. A. *J. Chem. Phys.* **2000**, *112*, 6532−6542.

(39) Martin, J. M. L.; de Oliveira, G. *J. Chem. Phys.* **1999**, *111*, 1843−1856.

(40) Frisch, M. J.; Trucks, G. W.; Schlegel, H. B.; Scuseria, G. E.; Robb, M. A.; Cheeseman, J. R.; Montgomery, J. A., Jr.; Vreven, T.; Kudin, K. N.; Burant, J. C.; Millam, J. M.; Iyengar, S. S.; Tomasi, J.; Barone, V.; Mennucci, B.; Cossi, M.; Scalmani, G.; Rega, N.; Petersson, G. A.; Nakatsuji, H.; Hada, M.; Ehara, M.; Toyota, K.; Fukuda, R.; Hasegawa, J.; Ishida, M.; Nakajima, T.; Honda, Y.; Kitao, O.; Nakai, H.; Klene, M.; Li, X.; Knox, J. E.; Hratchian, H. P.; Cross, J. B.; Bakken, V.; Adamo, C.; Jaramillo, J.; Gomperts, R.; Stratmann, R. E.; Yazyev, O.; Austin, A. J.; Cammi, R.; Pomelli, C.; Ochterski, J. W.; Ayala, P. Y.; Morokuma, K.; Voth, G. A.; Salvador, P.; Dannenberg, J. J.; Zakrzewski, V. G.; Dapprich, S.; Daniels, A. D.; Strain, M. C.; Farkas, O.; Malick, D. K.; Rabuck, A. D.; Raghavachari, K.; Foresman, J. B.; Ortiz, J. V.; Cui, Q.; Baboul, A. G.; Clifford, S.; Cioslowski, J.; Stefanov, B. B.; Liu, G.; Liashenko, A.; Piskorz, P.; Komaromi, I.; Martin, R. L.; Fox, D. J.; Keith, T.; M. A. Al-Laham, Peng, C. Y.; Nanayakkara, A.; Challacombe, M.; Gill, P. M. W.; Johnson, B.; Chen, W.; Wong, M. W.; Gonzalez, C.; , and Pople, J. A. *Gaussian 03, Revision C.02*; Gaussian, Inc., Wallingford, CT, 2004.

(41) Chan, B.; Radom, L. *J. Phys. Chem. A* **2012**, *116*, 4975−4986.

(42) Acetonitrile is a relatively strong HBA ($\beta_2^H = 0.44$).[28] However, the observation of very similar decay rate constants for CumO$^\bullet$ and BnO$^\bullet$ in acetonitrile (compare, for example, the intercepts of the plots displayed in Figure 1 and in the Supporting Information) clearly indicates that in these reactions BnO$^\bullet$/MeCN hydrogen bonding plays a negligible role. Previous studies have shown very similar rate constant ratios for hydrogen abstraction from propanal and THF (for which $\beta_2^H = 0.39$ and 0.51, respectively)[28] by CumO$^\bullet$ and BnO$^\bullet$ ((k_H(BnO$^\bullet$)/k_H(CumO$^\bullet$) = 1.2 and 1.3,[13,43] respectively), suggesting that the lower HBA ability of these substrates and of MeCN in comparison to that of tertiary alkylamines and alkanamides does not allow the formation of a sufficiently stable hydrogen-bonded prereaction complex.

(43) Bietti, M.; Martella, R.; Salamone, M. *Org. Lett.* **2011**, *13*, 6110−6113.

(44) Becke, A. D. *J. Chem. Phys.* **1993**, *98*, 5648−5652.

(45) Lee, C.; Yang, W.; Parr, R. G. *Phys. Rev. B* **1988**, *37*, 785−789.

(46) DCPs are atom-centered potentials that correct the long-range potential in which the electrons move and can be used with most versions of computational chemistry programs. A sample input file demonstrating the use of DCPs is given in the Supporting Information, and more information is available at www.ualberta.ca/~gdilabio.

(47) For clarity, binding energies refer to the difference between the electronic energies of the complex and the separated reactants and do not include zero-point energy. Inclusion of zero-point energy and vibrational enthalpy reduces BEs by ca. 1.5 kcal mol^{-1}.

(48) A less important abstraction pathway involving the prereaction complex in Figure 2b is that associated with the process illustrated by Figure 2b → Figure 2c. This process has a calculated energy (free energy) barrier of 7.3 (6.9) kcal mol^{-1}. To reach this TS requires stretching the (BnO$^\bullet$)OCH···O(DMF) hydrogen bond of the prereaction complex while forming a new (BnO$^\bullet$)HCO···HCN(DMF) hydrogen bond. Stacking interactions are maintained over the course of the reaction. The computed rate constant for this process is 5.9 × 10^7 s^{-1}.

(49) Johnson, R. A.; Nidy, E. G. *J. Org. Chem.* **1975**, *40*, 1680−1681.